

# Limits on methane release and generation via hypervelocity impact of Martian analogue materials

M. C. Price<sup>1</sup>, N. K. Ramkissoon<sup>1</sup>, S. McMahon<sup>2</sup>, K. Miljković<sup>3</sup>, J. Parnell<sup>2</sup>,  
P. J. Wozniakiewicz<sup>1,4</sup>, A. T. Kearsley<sup>4</sup>, N. J. F. Blamey<sup>5</sup>, M. J. Cole<sup>1</sup>  
and M. J. Burchell<sup>1</sup>

<sup>1</sup>School of Physical Sciences, University of Kent, Canterbury, Kent CT2 7NH, UK  
e-mail: mcp2@star.kent.ac.uk

<sup>2</sup>School of Geosciences, University of Aberdeen, Aberdeen AB24 3UE, UK

<sup>3</sup>Institut de Physique du Globe de Paris, Sorbonne Paris Cité, Université Paris Diderot, CNRS UMR7554, F-75005 Paris, France

<sup>4</sup>Department of Mineralogy, The Natural History Museum, South Kensington, London SW7 4BD, UK

<sup>5</sup>Department of Earth and Environmental Science, New Mexico Tech, 801 Leroy Place, Socorro, NM 87801, USA

**Abstract:** The quantity of methane in Mars' atmosphere, and the potential mechanism(s) responsible for its production, are still unknown. In order to test viable, abiotic, methanogenic processes, we experimentally investigated two possible impact mechanisms for generating methane. In the first suite of experiments, basaltic rocks were impacted at  $5 \text{ km s}^{-1}$  and the quantity of gases ( $\text{CH}_4$ ,  $\text{H}_2$ ,  $\text{He}$ ,  $\text{N}_2$ ,  $\text{O}_2$ ,  $\text{Ar}$  and  $\text{CO}_2$ ) released by the impacts was measured. In the second suite of experiments, a mixture of water ice,  $\text{CO}_2$  ice and anhydrous olivine grains was impacted to see if the shock induced rapid serpentinization of the olivine, and thus production of methane. The results of both suites of experiments demonstrate that impacts (at scales achievable in the laboratory) do not give rise to detectably enhanced quantities of methane release above background levels. Supporting hydrocode modelling was also performed to gain insight into the pressures and temperatures occurring during the impact events.

Received 7 July 2013, accepted 22 September 2013, first published online 13 November 2013

## Introduction

The existence, or non-existence, of methane on Mars is still a matter of debate (Formisano *et al.* 2004; Krasnopolsky *et al.* 2004; Mumma *et al.* 2009; Zahnle *et al.* 2011); a debate that NASA's *Mars Science Lander (MSL)* has contributed to by setting an upper limit of  $\sim 3.5$  ppbv at Gale Crater (Webster *et al.* 2013), although this limit does not yet rule out methane at levels compatible with previous claims (Hand 2012) in different locales, and/or due to seasonal variations. If methane is definitively discovered on Mars by *MSL*, as it progressively increases its sensitivity and as the seasons change, or by future missions such as ESA's *ExoMars Trace Gas Orbiter* (due for launch in 2016 and able to detect atmospheric methane down to a few parts per trillion), then the unanswered question still remains: where could the methane originate from?

The exciting answer to this question is a biological origin. However, before assuming an origin for which there is no other evidence, more routine geochemical paths need to be considered. One possible geochemical source is that the gas evolved during hypervelocity impacts. Impacts are on-going on Mars (e.g. Malin *et al.* 2006; Byrne *et al.* 2009), at a rate of  $\sim 40$  per year (Ivanov *et al.* 2010a) with impact speeds ranging from a few  $\text{km s}^{-1}$  (the Martian in-fall speed is  $5 \text{ km s}^{-1}$ ) to  $50 \text{ km s}^{-1}$  (Steel 1998). Additionally, impacts onto the northern hemisphere of Mars have exposed water ice under

the Martian regolith (Byrne *et al.* 2009; Dundas & Byrne 2010). It is thus clear that hypervelocity impacts occur, or have occurred, onto rock/ice mixtures, including intimate mixes of olivine family minerals (which are within the Martian regolith – Koeppen & Hamilton 2008) carbonates and ( $\text{CO}_2$  rich/pure) water ice. This raises the intriguing possibility of impact driven shock synthesis and/or alteration of minerals with subsequent release of methane. Therefore, we set out to investigate two questions:

- (1) Could contemporary impacts on Mars produce sufficient methane to explain the excess reported in its atmosphere, thus ruling out a biotic origin?
- (2) Can the quantity of any such methane (or other materials) produced be estimated given data regarding the current and past impact rate on Mars?

The answers to these questions would be a major contribution to the ongoing Mars methane debate. Two possible mechanisms were investigated looking for excess methane production: (i) evolution of methane from shock impacting basaltic rocks and, (ii) shock-induced serpentinization of a mix of water ice,  $\text{CO}_2$  ice and olivine grains.

Previous experiments have shown (McMahon *et al.* 2012) that an organic-rich impactor was able to increase the relative abundance of methane in a porous sandstone target. A natural extension of this work was to take some well-characterized basaltic rocks, known to contain varying quantities of

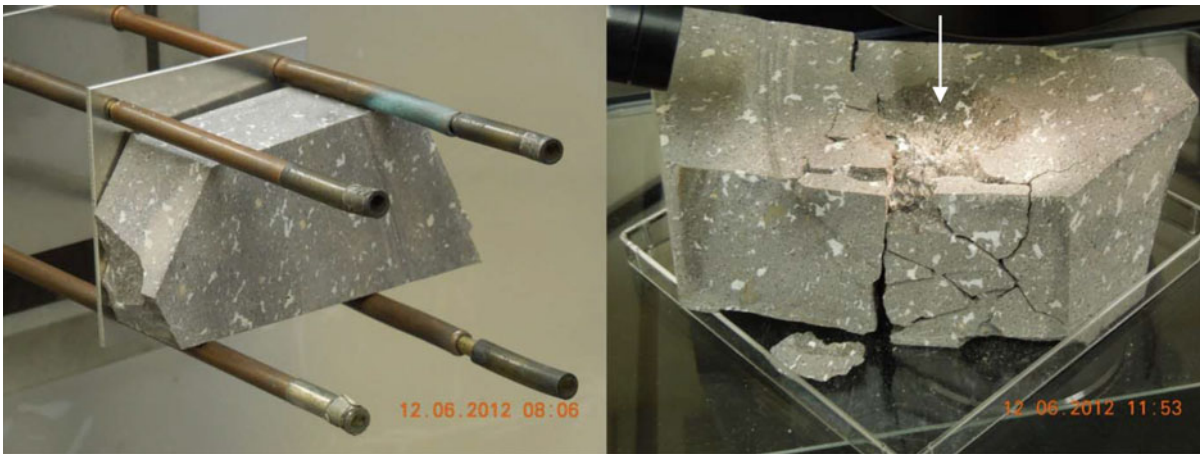


**Fig. 1.** Photographs of typical shot setup with sample ‘(iii)’ mounted in the LGG chamber prior to shooting (top) and after removal from the gun (bottom). The impact direction is shown arrowed in each image. For scale, the rock is  $\sim 100$  mm long, 80 mm wide and 60 mm deep. Note the corner of the rock has been removed (bottom left-hand corner) to give a pre-shocked sample to analyse. Post shot (right-hand panel) not only has a crater been formed (seen on the upper surface) but the extent of the subsurface damage can also be seen on the front face.

methane, and impact them with a stainless steel impactor to see if the shock changed the relative abundance of intrinsic methane within the rock. Impacts could therefore possibly generate atmospheric methane by releasing gas trapped in the underlying Martian basaltic lithology. To investigate if, and how much, gas may be released during such impacts we have taken three different types of basalt and fired projectiles at them in a light gas gun (LGG). The projectile impact speed was close to the Martian escape velocity of  $5 \text{ km s}^{-1}$ . Shocked and unshocked samples were then crushed and the evolved gases measured in a high-sensitivity mass spectrometer.

A second possible source of methane is through impact-induced serpentinization (where olivine reacts with water and carbolic acid to produce, among other products, serpentine and, in some reaction routes, methane). Again, to determine if this is a potentially viable process, Martian analogue soil mixtures of anhydrous olivine grains,  $\text{CO}_2$  and water ice were impacted and the ejecta collected. The recovered olivine grains were then examined using a Raman spectrometer to try and detect any signs of serpentine. Serpentine can be detected by the strong hydroxyl (OH) vibrational lines in Raman spectra at  $3670$  and  $3700 \text{ cm}^{-1}$ , (Auzende *et al.* 2004; Mouri & Enami 2008). Although  $\text{CO}_2$  ice is thought to only exist in substantial quantities at the Martian south pole (Phillips *et al.* 2011) carbonates have been detected at lower latitudes (Morris *et al.* 2010) and would release  $\text{CO}_2$  gas upon impact shocking, providing a secondary source of  $\text{CO}_2$  (Ivanov & Pierazzo 2011). Furthermore,  $\text{CO}_2$  gas could also be trapped in fissures and vesicles in the subsurface or simply be frozen into the subsurface water ice.

It is therefore possible that methane and/or magnesite could be produced in the Martian subsurface, potentially at significant distances from an impact point, due to shock wave propagation. Methane produced via this route could be trapped in the subsurface for long periods and does not require a hydrothermal production mechanism (such as described in Schwenzer & Kring 2009), whether contemporary or otherwise.

Table 1. Shot parameters. The projectile was a 2.5 mm diameter stainless steel-420 sphere for samples (i) and a 2.0 mm diameter sphere for samples (ii) and (iii)

Sample	Shot ID	$v$ ( $\text{km s}^{-1}$ )	$P_s$ (GPa)
(i)	G181111#1	4.69	116
(ii)	G120612#3	4.87	123
(iii)	G120612#2	4.74	118

## Experimental programme A: methane release from impacted basalts

### Methodology

Three different types of basalt were used in these experiments:

*Sample (i)* An intrusive basalt from Fife, Scotland.

*Sample (ii)* A recent Icelandic basalt from mid-Atlantic magmatic activity.

*Sample (iii)* A Devonian basalt from continental volcanic activity in Scotland.

Each sample was mounted (see example in Fig. 1) in the LGG at the University of Kent (Burchell *et al.* 1999) and fired into with a stainless steel projectile. The impact speed was measured in each shot to an accuracy of  $\pm 1\%$ . Table 1 gives a summary of the shots performed, and the approximate peak shock pressure,  $P_s$  (Pa), as calculated using the late stage effective energy method (LSEE), developed by Mizutani *et al.* (1990) and used by Burchell *et al.* (2004) and Parnell *et al.* (2010) to describe impacts in the Kent LGG, which gives:

$$P_s = \frac{mv}{2V_p} \left( C + \frac{sv}{2} \right) \quad (1)$$

where  $V_p$  and  $m$  are the projectile volume ( $4.19 \times 10^{-9} \text{ m}^3$  for a 2 mm diameter sphere;  $8.18 \times 10^{-9} \text{ m}^3$  for a 2.5 mm sphere) and mass ( $3.24 \times 10^{-5} \text{ kg}$  for a 2 mm diameter sphere;  $6.33 \times 10^{-5} \text{ kg}$  for a 2.5 mm diameter sphere), respectively,  $C$  ( $2600 \text{ m s}^{-1}$ ) and  $s$  (1.62) are the linear shock wave speed

Table 2. Measured values of gases evolved during the crush process. The percentages of each of the detected (above background) species are given. Numbers in '( )'s are standard deviations. 'Average burst' is the average signal current measured during each of the crushes, which is then converted into a total number of nano-moles of gas evolved

% abundance	(i) Basalt, Scotland		(ii) Recent basalt, Iceland		(iii) Devonian basalt, Scotland	
	Unshocked	Shocked	Unshocked	Shocked	Unshocked	Shocked
No. of crushes	6	6	5	6	3	4
CH <sub>4</sub>	1.1975 (1.198)	6.9886 (3.960)	4.042 (3.464)	3.923 (2.766)	4.113 (5.393)	4.028 (1.492)
H <sub>2</sub>	7.6305 (3.369)	16.385 (9.622)	5.443 (6.226)	6.169 (4.014)	12.797 (4.490)	17.393 (6.705)
He	0.0084 (0.002)	0.0142 (0.007)	0.013 (0.023)	0.012 (0.009)	0.119 (0.010)	0.161 (0.076)
N <sub>2</sub>	78.792 (12.31)	20.857 (11.01)	60.528 (14.76)	65.428 (9.113)	42.662 (1.354)	52.363 (0.9084)
O <sub>2</sub>	0.0674 (0.098)	0.0499 (0.025)	0.3290 (0.383)	0.0079 (0.336)	20.117 (1.621)	10.992 (2.953)
Ar	0.1497 (0.033)	0.2474 (0.123)	0.8050 (0.158)	0.817 (0.105)	0.593 (0.011)	0.604 (0.061)
CO <sub>2</sub>	12.154 (14.37)	55.458 (22.29)	28.841 (11.92)	23.573 (4.460)	19.598 (6.952)	14.459 (4.945)
Avg. Burst (amps)	$2.676 \times 10^{-7}$	$7.075 \times 10^{-8}$	$3.608 \times 10^{-8}$	$3.990 \times 10^{-8}$	$1.190 \times 10^{-7}$	$1.016 \times 10^{-7}$
Total gas evolved (nmols)	0.2539	0.0671	0.0342	0.0379	0.1129	0.0964

parameters for basalt (Melosh 1989) and  $v$  is the impact velocity ( $\text{m s}^{-1}$ ).

In each case, several grams of pre-shot material were kept to compare gas concentrations within the material before and after the shot. After shooting,  $\sim 0.1$  g samples were taken from the shocked regions within the impact craters and from the pre-shot material, crushed and analysed separately using Pfeiffer Prisma quadrupole mass spectrometers at New Mexico Tech. Several crushes per sample were performed to obtain some statistical data on the spread of the gas concentration within each sample (the exact number of crushes for each sample is given in Table 2). The sampling and analysis techniques are discussed in great detail in Norman & Moore (1997); Moore *et al.* (2001); Norman & Blamey (2001); Parry & Blamey (2010) and Blamey (2012).

## Results

Table 2 presents the relative abundances of each gas detected. It should be emphasized that crushing does not liberate all entrapped gases within the sample and the amount of fluid released varies with each crush (McMahon *et al.* 2012). Note that the abundance level of helium is very close to the detection limit of the analysis instrumentation, and therefore care must be taken in inferring any trend for the He data. There was no significant change in the relative abundance (within the experimental spread of data) for any gas within the rocks, including methane, with the exception of decreases in both N<sub>2</sub> in sample (i) and O<sub>2</sub> in all three of the samples.

## Hydrocode modelling

To try and understand why certain gases (such as N<sub>2</sub> and O<sub>2</sub>) appear to be released from the basalt, but others (such as methane) did not, hydrocode modelling was undertaken to give some insight into the pressure and temperatures experienced by the target during an impact. It may be that it requires a combination of high temperatures and pressures, held for a certain period of time, for a specific gas to be desorbed from the rock during the impact.

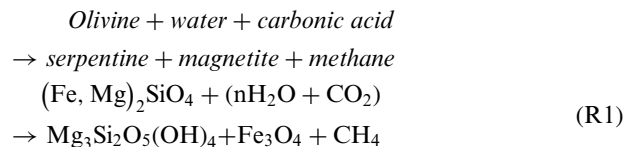
iSALE-2D (e.g. Amsden *et al.* 1980; Collins *et al.* 2004) is a multi-material and multi-rheology finite difference shock physics code used for simulating impact processes. The code has been benchmarked against other hydrocodes (Pierazzo *et al.* 2008) and validated against laboratory experiments (Davison *et al.* 2011). The target in iSALE-2D was modelled as a cylindrically symmetrical half-space mesh with the cell size of  $0.1 \text{ mm} \times 0.1 \text{ mm}$ . A material model for basalt composed of a Tillotson equation of state (Tillotson 1962), with parameters taken from Benz & Asphaug (1999) and the strength and damage model taken from Ivanov *et al.* (2010b), were used as target material properties.

Figure 2 shows the output from an impact simulation made by a 2 mm-metal projectile impacting vertically into the basalt target at  $5 \text{ km s}^{-1}$  impact speed. In each of the four panels (Fig. 2 (a)–(d)) the left half of the panel shows contours of pressure (Pa) and the right half contours are of temperature (K).

The simulations show that the peak pressure experienced was  $\sim 65 \text{ GPa}$  and a peak temperature of  $\sim 1600 \text{ K}$ . Although these values are high, they are only experienced in the target for  $\sim 100 \mu\text{s}$ , possibly insufficient time for desorption of trapped methane. For larger scale impacts, as modelled by Marinova *et al.* (2011), the timescales for which these pressures and temperatures are experienced increases as a function of the impactor size. Thus, for a 100 m diameter impactor, the high pressures and temperatures will persist for  $\sim 10\text{s}$  of seconds, possibly sufficient to cause significant outgassing of the target material. This could, potentially, be partially tested experimentally by flashing heating samples of basalt to temperatures, and for timescales, provided by the simulations.

## Programme B: Impact-induced serpentinization

Serpentine can be produced via:



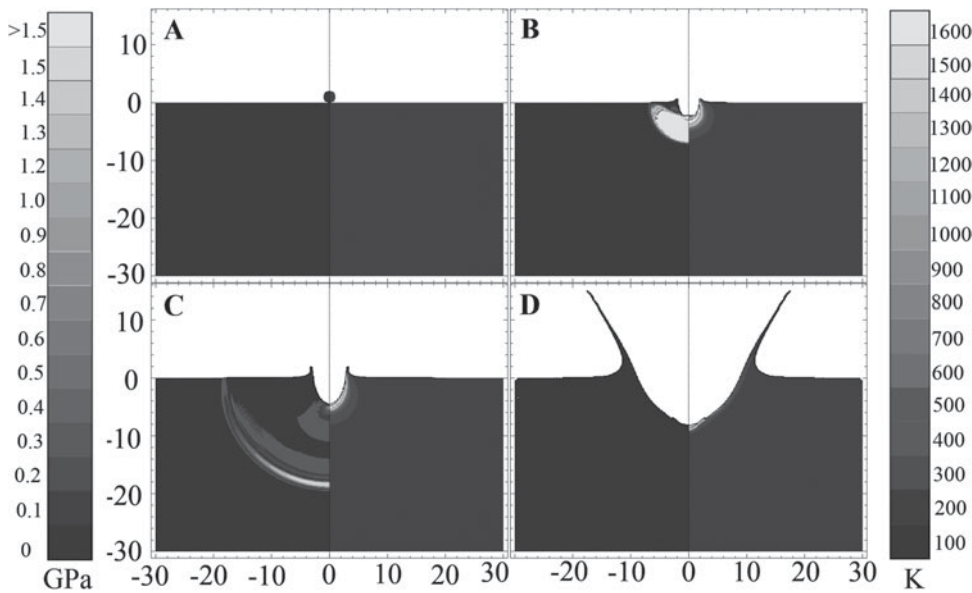
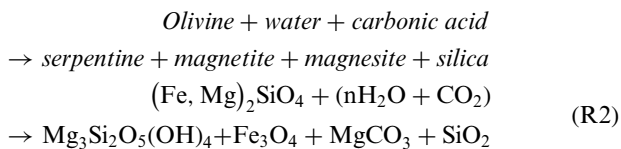


**Fig. 2.** iSALE hydrocode output showing contours of pressure and temperature as a function of time. (A):  $t=0 \mu\text{s}$ , (B):  $t=1 \mu\text{s}$ , (C):  $t=3 \mu\text{s}$ , (D):  $t=100 \mu\text{s}$ . Each panel ('A', 'B', 'C', 'D') is split into two halves: the left-hand half shows pressure (left-hand colour key), the right-hand half displays temperature (right-hand colour key). Dimensions along the  $X$ - and  $Y$ -axes are in millimetres. The impactor was a 2 m diameter stainless-steel sphere impacting at  $5 \text{ km s}^{-1}$  onto a basalt target.

and



Both methane and magnesite ( $\text{MgCO}_3$ ) are of astrobiological significance (Russell *et al.* 1999; Trieman *et al.* 2002). Shock production of either negates the necessity for a biological origin. For example, the possible identification of microbiota in ALH84001 (McKay *et al.* 1996) was supported by the discovery of carbonate globules. However, similar globules are produced in shock impacts (see Figure 2 from Lindgren *et al.* 2013) into calcite, and have also been observed in iron rich carbonates (Trieman 2003). Additional supporting work has shown that methane can be impregnated, and subsequently trapped, within a porous sandstone target by a hypervelocity impact from an organic-rich impactor (McMahon *et al.* 2012) indicating that there may be reservoirs of methane on Mars from historic impact of organic rich impactors.

### Methodology

Targets were made-up of a mixture of  $\text{CO}_2$ ,  $\text{H}_2\text{O}$  (ice) and olivine grains ( $>355 \mu\text{m}$  in diameter), with a 2:2:1 weight ratio, respectively. The olivine grains were baked in a furnace at  $600^\circ\text{C}$  for 12 h to remove any serpentinization which may have previously occurred. Heating the grains in air at  $600^\circ\text{C}$  causes the reaction below (Deer *et al.* 1992), which yields anhydrous olivine.



Crushed  $\text{CO}_2$  (sourced from 'BOC special gases', UK) and  $\text{H}_2\text{O}$  ice (made from filtered, reverse osmosis water) were mixed with the olivine grains (total mass 100 g, sourced from the Natural History Museum's (London) mineral collection), and the surface sprayed with high performance liquid chromatography grade (HPLC) water before being stored overnight in a freezer at  $-30^\circ\text{C}$  prior to the hypervelocity impact. Spraying the target with HPLC water prevents the target material crumbling when being placed into the horizontal target holder.

Four shots were made in this part of the programme. In each case the targets were impacted by a 2 mm diameter stainless steel sphere at velocities between 3 and  $6 \text{ km s}^{-1}$ . A four segment ejecta capture system (ECS) was used to collect ejected target material. Each segment (labelled ECS 1–ECS 4) of the ECS collects materials at different angles of ejection (ECS 1:  $0\text{--}25^\circ$ , ECS 2:  $50\text{--}65^\circ$ , ECS 3:  $65\text{--}75^\circ$  and ECS 4:  $75\text{--}85^\circ$  – see Fig. 3).

### Analysis

The impacted material recovered from each segment of the ECS, control, and the remaining target material within the target container, were placed into separate funnels onto clean filter paper and placed inside a fume cupboard. This allowed the olivine grains to be quickly separated from the  $\text{CO}_2$  and  $\text{H}_2\text{O}$  ice mixture, ensuring any serpentinization that may have occurred resulted from the impact alone. The grains were then left overnight in a fume cupboard to dry completely before analysis was carried out.

A Horiba LabRam-HR Raman spectrometer was used to determine if serpentinization had occurred in the

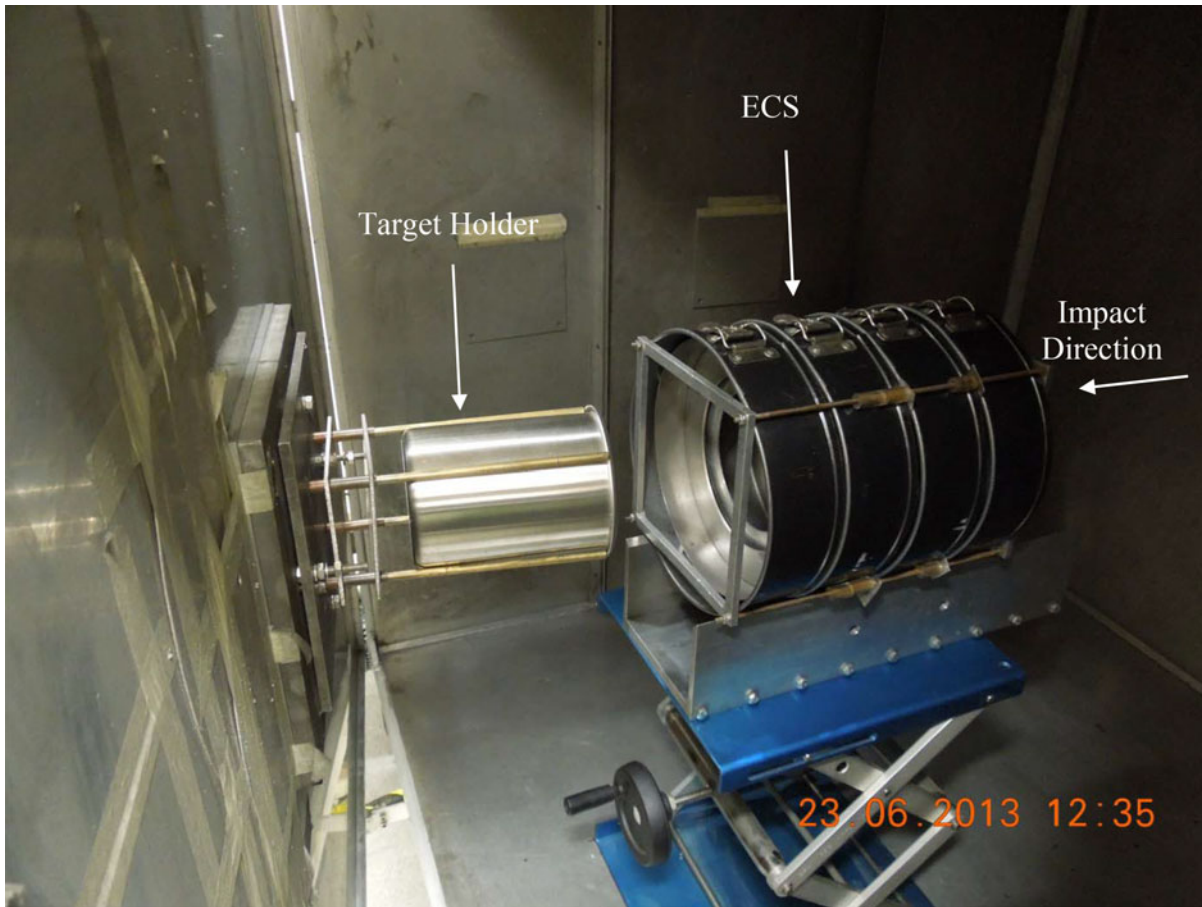


**Fig. 3.** Photograph of the ECS (right) and target holder (left) in the LGG target chamber. The projectile direction is from right  $\rightarrow$  left and the ejecta is contained within the four compartments of the capture system (ECS 1 is closest to the target). The capture system is then disassembled and the resulting ejecta removed. For scale, the length of the capture system is 271 mm and it has an outside diameter of 231 mm.

shocked olivine grains. The presence of a hydroxyl (OH) peak between  $3692$  and  $3710\text{ cm}^{-1}$  would indicate hydration had occurred, and therefore serpentinization, which would have released  $\text{CH}_4$  or  $\text{H}_2$  (depending on the reaction that took place).

Fifty grains were analysed from each segment of the ECS and the unshocked control sample to establish if there was a statistical difference in the quantity of grains (if any) that presented signs of serpentinization. Raman spectra of 50 pre-shocked olivine grains showed high Mg olivine, with a doublet peak at  $823$  and  $856\text{ cm}^{-1}$  (Kuebler *et al.* 2006), and had no detectable (above instrument noise) OH feature between  $3690$  and  $3710\text{ cm}^{-1}$ . In addition, grains were analysed from the remnant material in the target holder, although (due to sublimation of the  $\text{CO}_2$  ice) it is impossible to tell where such grains were in relation to the impact site. None of the grains taken from the shocked target container showed any signs of hydration.

Table 3 (below) gives calculations of the approximate peak shock pressures experienced by the olivine grains at the four impact velocities used here, as serpentinization is known to occur at pressures between  $0.1\text{ MPa}$  and  $1\text{ GPa}$  (Hyndman & Peacock 2003; Deangelis *et al.* 2010). The approximate shock pressures were calculated using equation (1), and shock wave

parameters for  $\text{CO}_2$  ice, water ice and olivine were taken from Zubarev & Telegin (1962), Bakanova *et al.* (1975) and Brown *et al.* (1987), respectively. In each impact the peak pressures well exceed the threshold for serpentinization.

Initially, a number of grains showed a strong, sharp peak within the range expected for serpentine at  $3673\text{ cm}^{-1}$ . However, closer examination of the spectra, and comparison with known standards, showed that these peaks were associated with either talc or actinolite, which were also found within olivine grains as inclusions prior to impact.

Post shot, two olivine grains (from G100513#2: ECS 2) showed a strong sign of hydration, possibly from serpentinization (Fig. 4). However, these were the only two occurrences to show serpentinization from any of the 200 grains collected from this investigation. The occurrence of only these two grains (out of 200 studied) indicates that any amount of serpentinization present is low or that there may have been some form of contamination that may have occurred within this particular set of grains from that section of the ECS.

### Hydrocode modelling

In a similar vein to the first suite of experiments, hydrocode modelling was performed in order to establish the approximate

Table 3. Calculated pressures and temperatures from AUTODYN, and pressures from equation (1)

Shot I.D	Velocity (km s <sup>-1</sup> )	Approximate peak shock pressure (GPa)*	Peak shock pressure (GPa, AUTODYN)	Peak temperature (K, AUTODYN)
G220313#1	3.90	85	26.8	756
G240413#1	4.97	124	41.7	1183
G100513#2	5.52	147	51.5	1467
G230513#1	5.82	160	56.4	1640

\* As calculated using equation (1) for a 2:2:1 mix of CO<sub>2</sub>, water ice and olivine.

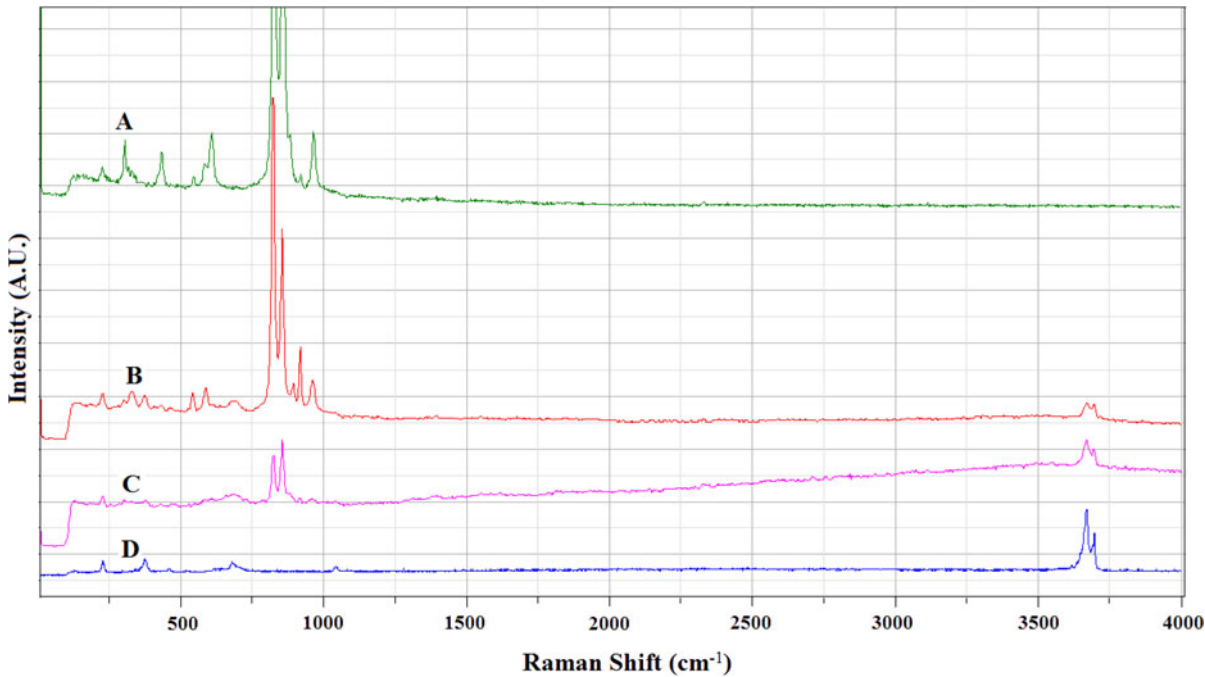


Fig. 4. Raman spectra of the two sampled hydrated olivine grains (B: red line, C: pink line) from G100513#2 ECS 2, compared with an unshocked olivine grain from the G100513#2 control sample (A: green line) and pure serpentine (D: blue line).

range of temperatures and pressures generated during the impact process. This is important, as the serpentinization reaction is a strong function of pressure and temperature (see for example, Berndt *et al.* 1996; Oze & Sharma 2007; Camille Jones *et al.* 2010; Schwenzer, 2011). The reaction rate the methane synthesis route R1 (above) increases by several orders of magnitude depending on the temperature, and also the presence of any surrounding metal particles (particularly nickel) which can catalyse the serpentinization reaction (Oze & Sharma 2005).

In order to simulate the impacts into ice, we used Ansys' AUTODYN hydrocode (Hayhurst & Clegg 1997) using a standard library material for the projectile (stainless-steel) and a 5-phase equation-of-state taken from Senft & Stewart (2008) for water ice and incorporated into AUTODYN via a user written subroutine. A simple Von Mises strength model was used for ice, using yield strength of 500 MPa, a shear modulus of 3.52 GPa and a tensile strength of 170 kPa.

Table 3 gives the peak pressures and temperatures for all four of the shots performed. Note that the pressure values calculated by AUTODYN are approximately less than 50%

of those calculated using equation (1). In Parnell *et al.* (2010) a comparison was made of peak pressures calculated by the LSEE (Equation (1)) and AUTODYN. It was found that the two approaches agreed well for limited regions in both projectile and target close to the contact plane, but that peak pressures fell rapidly inside the projectile at depth in the target. Specifically, the mean peak pressure found by AUTODYN in the leading half of the projectile was ~50% of that predicted by the LSEE method. Similarly, Parnell *et al.* found that at one projectile depth inside the target, the peak pressure had fallen by just over 50% from that at the surface. Thus while the LSEE gives a reasonable value of the peak pressure experienced by some materials in the impact, most of the shocked material experiences lower peak pressures.

## Discussion

Geminale *et al.* (2008) have estimated that the measured Martian atmospheric methane concentrations imply an annual influx of ~200 tonnes. Although the case for the presence of methane has not been universally accepted (Zahnle *et al.* 2011),

numerous plausible sources have now been proposed and discussed. Potential endogenous sources include serpentinization reactions, magmatic or hydrothermal fluid–rock interactions, and microbial activity (Oze & Sharma 2005; Lyons *et al.* 2005). Methane release could be mediated by the destabilization of clathrate hydrate deposits or desorption from mineral grains (Chastain & Chevrier 2007; Gough *et al.* 2010). However, there is no independent evidence for any of these activities on Mars; in particular, the Mars Odyssey thermal emission survey (THEMIS) found no evidence of magmatic or hydrothermal activity (Christensen *et al.* 2003).

Hence, exogenous sources must also be considered. Several mechanisms by which meteoritic material might contribute have now been investigated. Court & Sephton (2009) showed that the direct release of methane via the atmospheric ablation of organic-rich micrometeorites cannot supply the required flux. Krasnopolsky (2006) found that interplanetary dust, comets and meteorites could deliver only 6% of this flux. However, additional gas could be generated during impact events or by the photodegradation of meteoritic organics under ultraviolet radiation (Keppler *et al.* 2012).

Another possibility is that ancient methane trapped in rocks near the Martian surface is released during impact events. Using the techniques employed by the present study, McMahon *et al.* (2012) found that an organic-rich siltstone impactor was able to increase the relative abundance of methane in a porous sandstone target. In these experiments a 1.5 mm cube of organic rich Devonian siltstone from the Orcadian basin of northeast Scotland was fired at  $5 \text{ km s}^{-1}$  into a sandstone target (Triassic ‘Beestone’) known to be very low in intrinsic organics. Samples were taken from the resulting shocked target and the methane content measured. The  $\text{CH}_4/\text{CO}_2$  ratio of fluids released during subsequent crushing of these samples was higher than a control sample (unimpacted Beestone) and increased towards the crater centre, suggesting that a small amount of methane was impregnated from the organic-rich impactor into the target rock.

Therefore, it is possible that impact events may have injected methane into the Martian crust over geological time. Moreover, McMahon *et al.* (2013) found that methane was present in fluid inclusions or interstitial sites in a wide range of terrestrial basalts. This methane is likely to be the product of water–rock or hydrothermal fluid–rock reactions. If so, flood basalts on Mars might amount to a substantial methane reservoir. The Martian mantle is believed to be both more reducing and more iron-rich than the Earth’s and may therefore (a) equilibrate with more  $\text{CH}_4$ -rich hydrothermal fluids and (b) generate more methane by the serpentinization of FeO-rich minerals (Sleep *et al.* 2004; Lyons *et al.* 2005; Bridges & Warren 2006; Hirschmann & Withers 2008). Hence, typical Martian basalt may possibly be more methane-rich than typical terrestrial basalt.

Here, we have investigated: (a) whether hypervelocity impacts can release methane from basalt and, (b) whether shocked targets analogous to the Martian surface undergo rapid serpentinization. Although methane was present in all three basalt targets, it did not show a consistent pattern of

increase or depletion following impact. Hence, the hypothesis that significant quantities of methane might be released from impacted basalt during impact events is not supported (notwithstanding the possibility that Martian basalts may be rich in  $\text{CH}_4$  for the reasons mentioned above). Moreover, there was no compelling evidence of rapid serpentinization in the shocked basalt. However, this may not be surprising given the timescales (nanoseconds–microseconds) involved. Neubeck *et al.* (2011) discuss the formation process of methane due to weathering, and only detect methane (at temperatures between 30 and  $70^\circ\text{C}$ ) after a couple of hundred days under (Earth) atmospheric pressure. Again, as with the impacts into basalt, it may be that at the sizes achievable in the laboratory, that timescales are too short (even under high temperatures and pressures) for any serpentinization reaction to begin. Larger scale modelling could provide some insight into the process, as well as adding chemical reactions into the hydrocode in an attempt to predict the possible quantities of methane produced. Finally, it is possible that methane could be produced due to the vaporization of the  $\text{CO}_2$  and water ice. The energy of the impact generates a plasma above the target, and recombination reactions between the ionized H and C within this plasma could provide a route for the synthesis of methane. However, to date, no experiments have been performed to investigate this theory.

## Conclusions

The first set of experiments suggest that under the impact conditions we can achieve with a typical LGG ( $\sim 100 \text{ GPa}$  at impact speeds of  $\sim 5 \text{ km s}^{-1}$  with mm sized projectiles), methane is not released at a level which significantly depletes the methane content of the basalt. This implies that any methane that may be confirmed on Mars is therefore not due to release from impacts onto basaltic bedrocks, although basalts are known to be methane bearing (McMahon *et al.* 2013). However, the data do show that other volatiles (here  $\text{N}_2$  and  $\text{O}_2$ ) may be released during impacts which could add to the atmospheric and surface chemistry.

The second series of hypervelocity impacts conducted showed no statistically significant sign of impact induced hydration, and thus rapid serpentinization, which could produce methane, although there was a small positive result in one experiment. This suggests that the quantity of serpentine produce from hypervelocity impacts is (at best) very small, and that higher velocities are required to generate higher pressures, or that rapid serpentinization of olivine does not occur. It does not however rule out shock induced serpentinization which could occur from larger impacts, which would cause elevated pressures and temperatures on longer timescales.

## Acknowledgements

The researchers at Kent acknowledge the STFC, UK for funding this work. Nisha Ramkissoon thanks the UK Space Agency for her support via an *Aurora* studentship. KM’s work is funded by the UnivEarthS LabEx project of the University of Sorbonne Paris Cité.

## References

- Amsden, A.A., Ruppel, H.M. & Hirt, C.W. (1980). SALE: a simplified ALE computer program for fluid flow at all speeds. *Los Alamos National Laboratories Report LA-8095*, 105.
- Auzende, A.L., Daniel, I., Reynard, B., Lemaire, C. & Guyot, F. (2004). High-pressure behavior of serpentine minerals: a Raman spectroscopic study. *Phys. Chem. Min.* **31**, 269.
- Bakanova, A.A., Zubarev, V.N., Sutulov Yu, N. & Trunin, R.F. (1975). Thermodynamic properties of water at high pressures and temperatures. *Zh. Eksp. Teor. Fiz.* **68**(3), 1099–1107 [in Russian]. Data taken from rusbank.ru (accessed 21st June 2013).
- Benz, W. & Asphaug, E. (1999). Catastrophic disruptions revisited. *Icarus* **152**, 5.
- Berndt, M.E., Allen, D.E. & Seyfried, W.E. (1996). Reduction of CO<sub>2</sub> during serpentinization of olivine at 300 °C and 500 bar. *Geology* **24**, 351.
- Blamey, N.J.F. (2012). Composition and evolution of crustal, geothermal and hydrothermal fluids interpreted using quantitative fluid inclusion gas analysis. *J. Geochem. Explor.* **116**, 17.
- Bridges, J.C. & Warren, P.H. (2006). The SNC meteorites: basaltic igneous processes on Mars. *J. Geol. Soc.* **163**, 229–251.
- Brown, J.B., Furnish, M. D. & McQueen, R.G. (1987). Thermodynamics for (Mg, Fe)<sub>2</sub>SiO<sub>4</sub> from the Hugoniot. In *High-Pressure Research in Mineral Physics*, eds Manghnani, M.H. & Syono, Y., pp. 373–384. AGU, Washington, DC.
- Burchell, M.J., Cole, M.J., McDonnell, J.A.M. & Zarnecki, J.C. (1999). Hypervelocity impact studies using the 2 MV Van de Graff accelerator and two-stage light gas gun at the University of Kent at Canterbury. *Meas. Sci. Technol.* **10**, 41.
- Burchell, M.J., Mann, J.R. & Bunch, A.W. (2004). Survival of bacteria and spores under extreme shock pressures. *Mon. Not. R. Astron. Soc.* **352**, 1273.
- Byrne, S. *et al.* (2009). Distribution of mid-latitude ground ice on Mars from new impact craters. *Science* **325**, 1674.
- Camille Jones, L., Rosenbauer, R., Goldsmith, J.I. & Oze, C. (2010). Carbonate control of H<sub>2</sub> and CH<sub>4</sub> production in serpentinization systems at elevated P-Ts. *Geophys. Res. Lett.* **37**, L14306.
- Chastain, B.K. & Chevrier, V. (2007). Methane clathrate hydrates as a potential source for Martian atmospheric methane. *Planet. Space Sci.* **55**, 1246–1256.
- Christensen, P.R. *et al.* (2003). Mars: Mars Odyssey THEMIS Results. *Science* **300**, 2056.
- Collins, G.S., Melosh, H.J. & Ivanov, B.A. (2004). Damage and deformation in numerical impact simulations. *Meteoritics Planet. Sci.* **39**, 217.
- Court, R.W. & Sephton, M.A. (2009). Investigating the contribution of methane produced by ablating micrometeorites to the atmosphere of Mars. *Earth Planet. Sci. Lett.* **288**, 382.
- Davison, T.M., Collins, G.S., Elbeshausen, D., Wünnemann, K. & Kearsley, A.T. (2011). Numerical modeling of oblique hypervelocity impacts on strong ductile targets. *Meteoritics Planet. Sci.* **46**, 1510.
- Deangelis, M.T., Labotka, T.C., Cole, D.R. & Fayek, M. (2010). Aqueous dissolution and alteration of olivine in low temperature and pressure environments. *GSA Denver Annual Meeting, Paper No. 135–12*.
- Deer, W.A., Howie, R.A. & Zussman, Z. (1992). *An Introduction to the Rock Forming Minerals*, 2nd edn. Longman Scientific and Technical, England.
- Dundas, C.M. & Byrne, S. (2010). Modeling sublimation of ice exposed by new impacts in the Martian mid-latitudes. *Icarus* **206**, 716.
- Formisano, V., Atreya, S., Encrenaz, T., Ignatiev, N. & Giuranna, M. (2004). Detection of methane in the atmosphere of Mars. *Science* **306**, 1758.
- Geminale, A., Formisano, V. & Giuranna, M. (2008). Methane in Martian atmosphere: average spatial, diurnal and seasonal behavior. *Planet. Space Sci.* **56**, 1194.
- Gough, R.V., Tolbert, M.A., McKay, C.P. & Toon, O.B. (2010). Methane adsorption on a Martian soil analog: an abiogenic explanation for methane variability in the Martian atmosphere. *Icarus* **207**, 165–174.
- Hand, E. (2012). Hopes linger for Mars methane. *Nature* **491**(7423), 174.
- Hayhurst, C.J. & Clegg, R.A. (1997). Cylindrically symmetric SPH simulations of hypervelocity impacts on thin plates. *Int. J. Impact Eng.* **20**(1–5), 337–348.
- Hirschmann, M.M. & Withers, A.C. (2008). Ventilation of CO<sub>2</sub> from a reduced mantle and consequences for the early Martian greenhouse. *Earth Planet. Sci. Lett.* **270**, 147–155.
- Hyndman, R.D. & Peacock, S.M. (2003). Serpentinization of the forearc mantle. *Earth Planet. Sci. Lett.* **212**, 417–432.
- Ivanov, B.A. & Pierazzo, E. (2011). Impact cratering in H<sub>2</sub>O-bearing targets on Mars: thermal field under craters as starting conditions for hydrothermal activity. *Meteoritics Planet. Sci.* **46**, 601.
- Ivanov, B.A., Melosh, H.J. & McEwen, A.S. (2010a). New small impact craters in high resolution HiRISE images – III. LPSC XLI, abstract #2020.
- Ivanov, B.A., Melosh, H.J. & Pierazzo, E. (2010b). Basin-forming impacts: reconnaissance modeling. In *Large Meteorite Impacts and Planetary Evolution IV*, eds Gibson, R.L. & Reimold, W.U., pp. 29–49, Special paper 465. Geological Society of America, Boulder, Colorado.
- Keppler, F., Vigano, I., McLeod, A., Ott, U., Früchtl, M. & Röckmann, T. (2012). Ultraviolet-radiation-induced methane emissions from meteorites and the Martian atmosphere. *Nature* **486**, 93.
- Koeppen, W.C. & Hamilton, V.E. (2008). Global distribution, composition, and abundance of olivine on the surface of Mars from thermal infrared data. *J. Geophys. Res.* **113**, E05001.
- Krasnopolsky, V.A. (2006). Some problems related to the origin of methane on Mars. *Icarus* **180**, 359.
- Krasnopolsky, V.A. *et al.* (2004). Detection of methane in the Martian atmosphere: evidence for life? *Icarus* **172**, 537.
- Kuebler, K.E., Jolliff, B.L., Wang, A. & Haskin, L.A. (2006). Extracting olivine (Fo – Fa) compositions from Raman spectral peak positions. *Geochem. Cosmochem. Acta* **70**, 6201.
- Lindgren, P. *et al.* (2013). Constraining the pressure threshold of impact induced calcite twinning: implications for the deformation history of aqueously altered carbonaceous chondrite parent bodies. *Earth Planet. Sci. Lett.* (accepted).
- Lyons, J.R., Manning, C. & Nimmo, F. (2005). Formation of methane on Mars by fluid-rock interaction in the crust. *Geophys. Res. Lett.* **32**, L131201.
- Malin, M.C., Edgett, K.S., Posiolova, L.V., McColley, S.M. & Noe Dobrea, E.Z. (2006). Present-day impact cratering rate and contemporary gully activity on Mars. *Science* **314**, 5805, 1573–1577.
- Marinova, M.M., Aharonson, O. & Asphaug, E. (2011). Geophysical consequences of planetary-scale impacts into a Mars-like planet. *Icarus* **211**, 960.
- McKay, D.S. *et al.* (1996). Search for past life on Mars: possible relic biogenic activity in Martian meteorite ALH84001. *Science* **273**, 924.
- McMahon, S., Parnell, J., Burchell, M.J. & Blamey, N.J.F. (2012). Methane retention by rocks following simulated impacts: implications for Mars. LPSC XXXXIII, abstract #1040.
- McMahon, S., Parnell, J. & Blamey, N.J.F. (2013). Sampling methane in basalt on Earth and Mars. *Int. J. Astrobiol.* **12**(2), 113–122.
- Melosh, H.J. (1989). Impact cratering: a geological process. *Oxford Monogr. Geol. Geophys.*
- Mouri, T. & Enami, M. (2008). Raman spectroscopic study of olivine-group minerals. *Journal of Mineralogical and Petrological Sciences* **103**, 100–104.
- Moore, J.N., Norman, D.I. & Mack Kennedy, B. (2001). Fluid inclusion gas compositions from an active magmatic-hydrothermal system. *Chem. Geol.* **173**, 3.
- Morris, R.V. *et al.* (2010). Identification of carbonate-rich outcrops on Mars by the Spirit rover. *Science* **329**, 421.
- Mizutani, H., Takagi, Y., Kawakami, S. (1990). New scaling laws on impact fragmentation. *Icarus* **87**, 307–326.
- Mumma, M.J. *et al.* (2009). Strong release of methane on Mars in northern summer 2003. *Science* **323**, 1041.
- Norman, D.I. & Blamey, N.J.F. (2001). Quantitative analysis of fluid inclusion volatiles by a two quadrupole mass spectrometer system. *Eur. Curr. Res. Fluid Inclusion*, **XVI**, 341.

- Norman, D.I. & Moore, J.N. (1997). Gaseous species in fluid inclusions: a fluid tracer and indicator of fluid processes. *Eur. Curr. Res. Fluid Inclus.*, **XIV**, 243.
- Neubeck, A. et al. (2011). Formation of H<sub>2</sub> and CH<sub>4</sub> by weathering of olivine at temperatures between 30 and 70 °C. *Geochem. Trans.* **12**, 6.
- Oze, C. & Sharma, M. (2005). Have olivine, will gas: Serpentinization and the abiogenic production of methane on Mars. *Geophys. Res. Lett.* **32**, L10203.
- Oze, C. & Sharma, M. (2007). Serpentinization and the inorganic synthesis of H<sub>2</sub> in planetary surfaces. *Icarus* **187**, 557.
- Parnell, J., Bowden, S., Lindgren, P., Burchell, M.J., Milner, D., Baldwin, E. C. & Crawford, I.A. (2010). The preservation of fossil biomarkers during hypervelocity impact experiments using organic rich siltstones as both projectiles and targets. *Meteoritics Planet. Sci.* **45**, 1340.
- Parry, W.T. & Blamey, N.J.F. (2010). Fault fluid composition from fluid inclusion measurements, Laramide age Uinta thrust fault, Utah. *Chem. Geol.* **278**, 105.
- Phillips, R.J. et al. (2011). Massive CO<sub>2</sub> ice deposits sequestered in the South polar layered deposits of Mars. *Science* **332**, 6031, 838.
- Pierazzo, E., et al. (2008) Validation of numerical codes for impact and explosion cratering: impacts on strengthless and metal targets. *Meteoritics Planet. Sci.* **43**, 1917.
- Russell, M.J. et al. (1999). Search for signs of ancient life on Mars: expectations from hydromagnesite microbialites, Salda Lake, Turkey. *J. Geol. Soc. (Lond.)* **156**, 869.
- Schwenzer, S.P. (2011). Quantifying low temperature production of methane on Mars. LPSC XXXXII, abstract # 1803.
- Schwenzer, S.P. & Kring, D.A. (2009). Impact-generated hydrothermal systems capable of forming phyllosilicates on Noachian Mars. *Geology* **37**(12), 1091.
- Senft, L.E. & Stewart, S.T. (2008). Modeling the morphological diversity of impact craters on icy satellites. *Meteoritics Planet. Sci.* **43**, 1993.
- Sleep, N., Meibom, A., Fridriksson, Th., Coleman, R.G. & Bird, D.K. (2004). H<sub>2</sub> rich fluids from serpentinization: Geochemical and biotic implications. *Proc. Natl. Acad. Sci. USA* **101**, 12818–12823.
- Steel, D. (1998). Distributions and moments of asteroid and comet impact speeds upon the Earth and Mars. *Planet. Space Sci.* **46**, 473.
- Tillotson, J.H. (1962). *Metallic Equations of State for Hypervelocity Impact. GA-3216, General Atomic, San Diego.*
- Trieman, A.H. (2003). Submicron magnetite grains and carbon compounds in Martian meteorite ALH84001: inorganic, abiotic formation by shock and thermal metamorphism. *Astrobiology* **3**, 369.
- Trieman, A.H., Amundsen, H.E.F., Blake, D.F. & Bunch, T. (2002). Hydrothermal origin for carbonate globules in Martian meteorite ALH84001: a terrestrial analogue from Spitsbergen (Norway). *Earth Planet. Sci. Lett.* **204**, 323.
- Webster, C.R. et al. (2013). Measurements of Mars methane at Gale crater by the SAM tuneable laser spectrometer on the Curiosity rover. LPSC XXXXIV, abstract # 1366.
- Zahnle, K., Freedman, R.S. & Catling, D.C. (2011). Is there methane on Mars? *Icarus* **212**, 493–503.
- Zubarev, V.N. & Telegin, G.S. (1962). Shock compressibility of liquid nitrogen and solid carbon dioxide. *Dokl. Akad. Nauk SSSR* **142**(2), 309 [in Russian]. Data taken from rusbank.ru (accessed 21st June 2013).